HEV series architectures evaluation: modeling, simulation and experimentation

David Bouquain, Benjamin Blunier and Abdellatif Miraoui
Transport and Systems Laboratory (SeT) – EA 3317/UTBM
University of Technology of Belfort-Montbéliard, France
Email: (david.bouquain,benjamin.blunier,abdellatif.miraoui)@utbm.fr

Abstract

This paper present a simulation and experimental comparison study of three HEV series architectures: engine only, battery hybridization and battery-ultracapacitors hybridization configurations. The models of the components, including vehicle, batteries, ultracapacitors, motor, generator and engine are introduced. Simulation and experimental results show that the fuel economy in the battery hybridization configuration is about 17 % compared to the engine stand-alone solution. Despite the battery-ultracapacitors hybridization configuration does not add significant fuel economy, it is shown that the battery transients can be limited to improve their lifetime. Simulation and experimental comparison show that the models permit the energy management strategies to be evaluated with a good accuracy before testing them on the real test bench.

Index Terms

Hybrid electric vehicle, energy storage, internal combustion engine, fuel economy

I. Introduction

Hybrid and electric vehicles (HEV) are made of different components and subsystems.

- the energy sources with their storage and conversion system;
- the engine and electric motors;
- the mechanical drives (i.e. gearbox) or static converters;
- the control and management of the different components (command tools, electronic boards, DC power bus and numerical network).

Each component has its own physics and a specified dynamic. So it is necessary to model and simulate the components with appropriate conditions.

The System and Transport laboratory (SeT) at the University of Technology of Belfort-Montbéliard (UTBM) has developed a modular test bench shown in Figure 1 in order to evaluate the different new technologies electric and hybrid power trains. The bench must be used for the validation and the tunning of design models and control laws. The expected modularity of all the components of the electric and hybrid power trains and the developed control strategies can be validated and improved using this tests bench.

In order to have a tests bench representative of a real vehicle, we have chosen to use 1:4 scale components (i.e., a 5 kW vehicle).

Many design can be tested as electrical, series and parallel architectures. With each of those architectures, it is possible to use one or some sources with many configurations; actually, 32 different configurations can be tested.

The paper is organized as follow: in a first part, an overview of the different investigated architectures is given: engine only, battery hybridization and supercapacitor-battery hybridization. The second part introduce the modelling of some of the components of the bench. The last part gives the simulation and experimentation results.

II. Investigated architectures

A. Engine and generator only

In this case, the diesel engine (connected with the generator) gives the energy needed by the load. The figure 3 shows the system control. The current reference of the generator AC-DC is the current used by the electric motor. A saturation function is used to protect the generator against overloads. The battery is only used for the fast transient phase and for the energy recovery during the braking periods.

B. Battery hybridization

The main advantage of hybrid vehicles is to optimize the fuel enconomy. The transients (acceleration, braking) need or give peaks of power. If theses transients are smoothed by using an auxiliary source (peaking power source), it is possible to improve the fuel economy and to downsize the engine as it does not need to give the maximum power.

The control strategy permits to use more the battery during the transient phases (figure 4). A first order transfer function is used to filter the generator current reference.

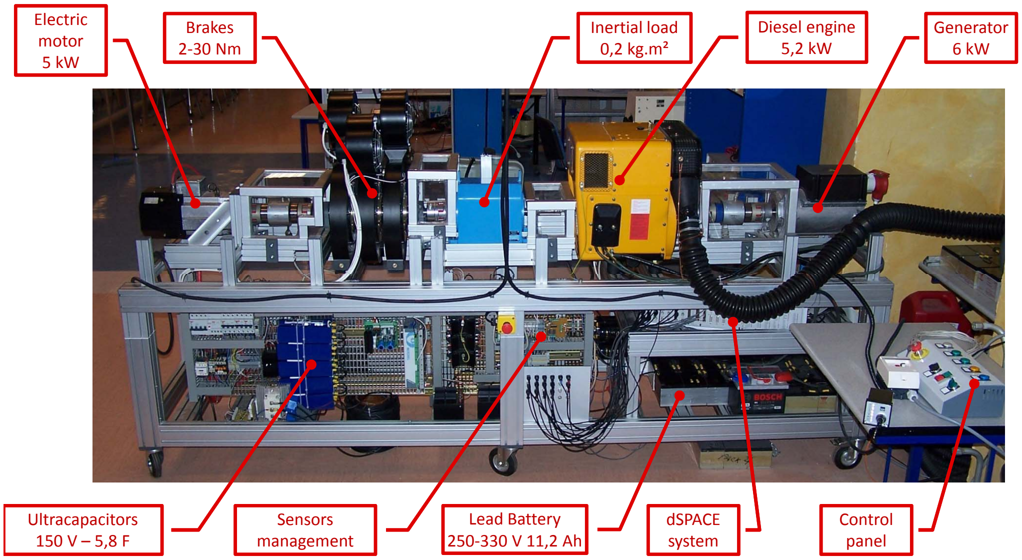

Figure 1. Hybrid test bench

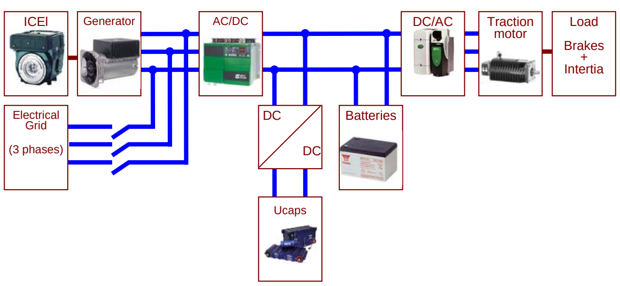

(a) Electrical and series configuration

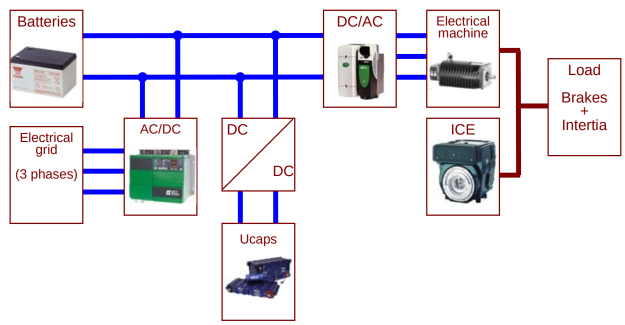

(b) Parallel configuration

Figure 2. Seial architecture

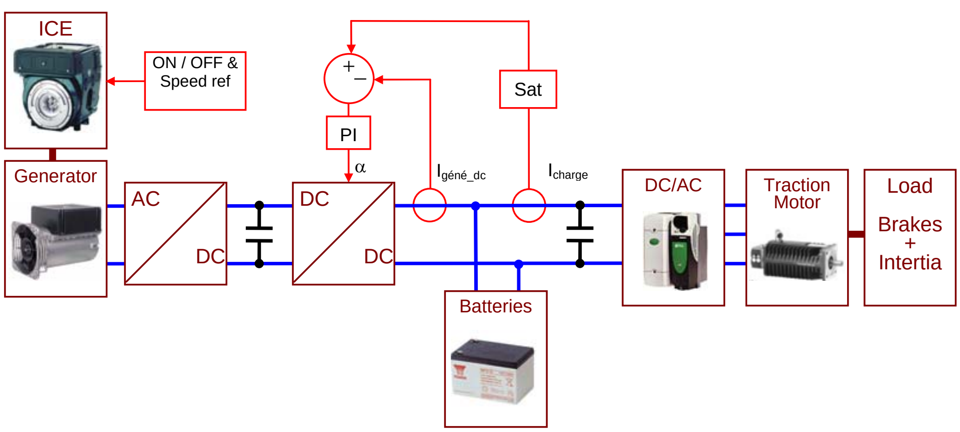

Figure 3. Control of the thermal generator

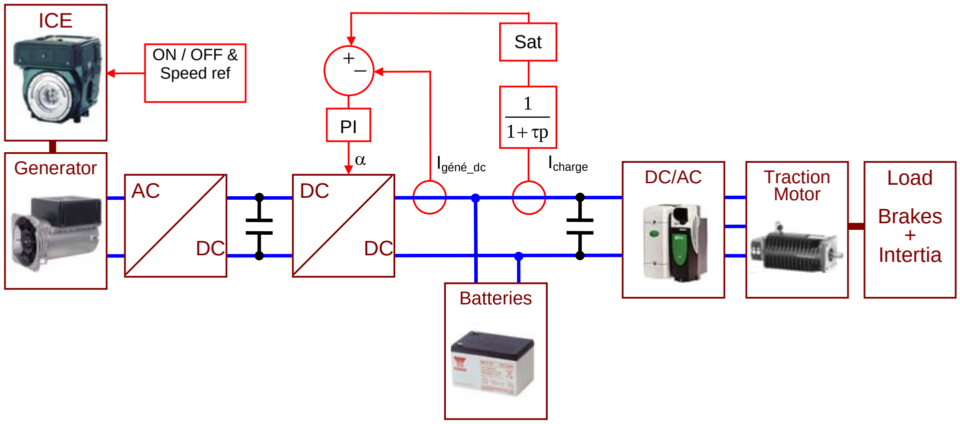

Figure 4. Engine control with battery hybridization

C. Ultracapacitors and battery hybridization

Ultracapacitors have been used to give (or to recover) power during the transient phases. The ultracapacitors are the best components for this kind of application as they offer a very high power density. The control strategy is shown on figure 5. A first order transfer function is used to generate the ultracapacitors current reference. The current of the AC-DC converter of the generator is the difference between the load current and the ultracapacitors current reference. The time constant of the transfer function can be adjusted to the desired dynamic.

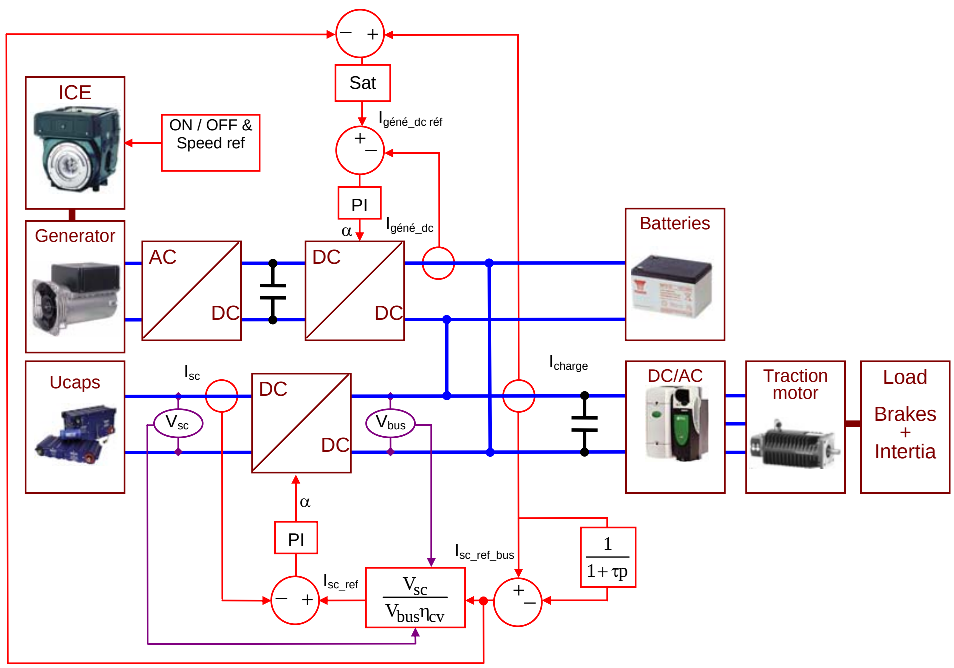

Figure 5. Engine control with battery and ultracapacitors hybridization

III. Components modeling

A. Vehicle mechanical model

The model of the vehicle is based on the mechanical forces acting on the vehicle. The electrical power (P_e) takes into account the dynamics of the vehicle (dv/dt), the speed v, the road grade (α), its total mass (M_v), the aerodynamic drag coefficient (C_x), the vehicle front surface including the driver (S), the rolling coefficient (C_r), the drive train efficiency (η_d) [1], [2].

$$P_{\mathrm{e}} = \frac{v}{\eta_d} \left(M_{\mathrm{v}} \frac{\mathrm{d}v}{\mathrm{d}t} + \frac{1}{2} \rho_{\mathrm{air}} v^2 S C_{\mathrm{x}} + M_{\mathrm{v}} g \sin\alpha + M_{\mathrm{v}} g C_{\mathrm{r}} \cos\alpha \right) \quad (1)$$

For a given driving cycle (speed and road grade profiles), the vehicle power can be computed from (1). The total nominal power of the investigated vehicle on the test bench is arround 5 kW.

B. Thermal engine model

The 5 kW internal combustion engine (ICE) model is based on a semi-empirical mean-value model given and described by [3], [4].

When the ICE is in steady state, two normalized variables can be used to describe the operating point [3]–[5]. This two variables are the *mean piston speed*

$$c_m = \frac{\omega_e S}{\pi} \quad (2)$$

and the *mean effective pressure*

$$p_{me} = \frac{N \pi T_e}{V_d} \quad (3)$$

where ω_e and T_e are the engine speed and torque, respectively. V_d is the engine displacement, S is its stroke. The parameter N depends on the engine type: for a four-strokes engine, $N = 4$ and for a two-strokes engine $N = 2$.

For the studied engine, $c_m = 6,5$ m/s.

The thermodynamic efficiency of an engine is the ratio between the mechanical power and the enthalpy flow (P_c) associated with the fuel mass flow $\dot{m}_f$:

$$\eta_e = \frac{\omega_e T_e}{P_c} \quad (4)$$

and

$$\dot{m}_f = \frac{P_c}{H_l} \quad (5)$$

where H_l is the fuel lower heating value.

The engine efficiency η_e mainly depedns on the speed (ω_e) and the torque (T_e). It is defined as follow:

$$\eta_e = f(\omega_e, T_e). \quad (6)$$

A very simple but useful approximation approximation, especially for diesel engines is the Willans description [4]. In this approximation, the engine mean effective pressure is approximated by

$$p_{me} \approx e(\omega_e) \cdot p_{mf} - p_{me0}(\omega_e) \quad (7)$$

where the input p_{mf} is the fuel mean effective pressure. This variable is the mean effective pressure that an engine with 100 % efficiency would produce by burnging a mass m_f of fuel with a (lower) heating value H_l

$$p_{mf} = \frac{H_l m_f}{V_d} \quad (8)$$

From this aproximation, another engine efficiency description can be obtained:

$$\eta_e = \frac{p_{me}}{p_{mf}} \quad (9)$$

The parameter $e(\omega_e)$ represents the thermodynamic efficiency, that is, the efficiency of the conversion of the fuel chemical energy to pressure inside the cylinder. The parameter p_{me0} summarize all the other losses (frictions).

Both of the parameter e and p_{me0} mainly depend on the engine speed; they are often approximated by splines or polynomes. For simple models these two parameters can be considered as constants.

The parameter e in this model is constant; a more complete formulation is given in [3]. The parameter p_{me0} is decompsed in two parts:

$$p_{me0} = p_{me0f} + p_{me0g} \quad (10)$$

where p_{me0g} is the cycle-averaged pressure difference between the intake and exhaust port of the engine; it is considered constant in this model. p_{me0f} represents the engine friction and are calculated as follow [6] :

$$p_{me0f} = k_1\left(\theta_e\right) \cdot \left(k_2 + k_3 \cdot S^2 \cdot \omega_e\right) \cdot \Pi_{e,max} \cdot \sqrt{\frac{k_4}{B}} \tag{11}$$

Typical values for the parameters of (11) for a diesel engine are given by the Table I. The variable $\Pi_{e,max}$ is the maximum boost ratio for which the engine is designed to operate at low speeds, B is the engine's bore diameter and S its stroke. The temperature dependance $k_1(\theta_e)$ is not considered (steady state) that is, $k_1 = \text{constant} = k_1(\theta_\infty)$.

	SI
$k_1(\theta_\infty)$	$1,44 \cdot 10^5$ (Pa)
k_2	$0,46$ (–)
k_3	$9,1 \cdot 10^{-4}$ (s²/m²)
k_4	$0,075$ (m)

Table I
FRICTION MODEL PARAMETERS FOR A DIESEL ENGINE [3]

The simplified representation (does not contain the engine limits) of the engine is given in figure 6.

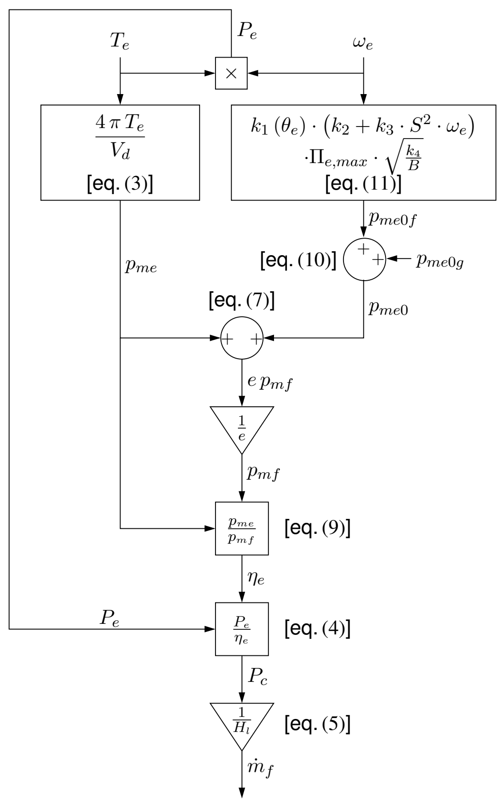

Figure 6. Engine model summary

The model validation against the manufacturer data is given by the figure 7(a). The engine efficiency map is given by the figure 7(b).

C. Electrical drives

The electric drives can be modeled using physical equation or directly based on experimental data. The objective of the model is to predict the operating point of the electrical drive, that is, the electrical machine together with its power converter.

The proposed method is based on the Willans approximation given in [4]. This model is very similar to that of the internal combustion engine:

$$P_{out} = e \cdot P_{in} - P_0 \tag{12}$$

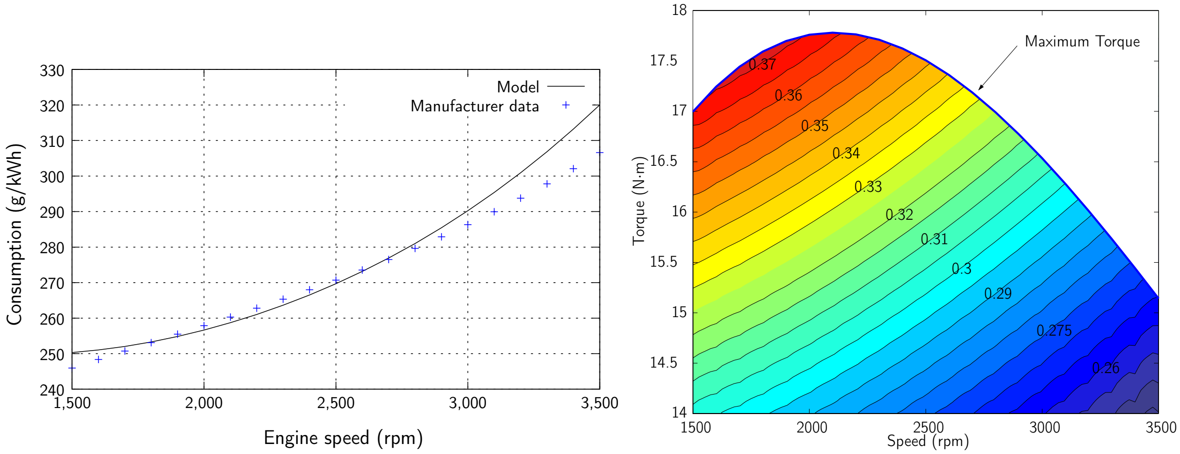

(a) Model validation at maximum torque

(b) Iso-efficiency map of the ICE

Figure 7. Engine model results

where P_{out} is the output power (mechanical power if it is motor and electrical power if it is a generator), P_{in}, is the input power (mechanical power if it is a generator and electrical power if it is a motor).

The electrical power includes the power converter. P_0 represents the losses after the energy conversion and e is the maximum efficiency which can be achieved, that is when $P_0 = 0$. The total efficiency η_m takes into account P_0.

This model, even it is very simple, is very accurate to predict the different operating points of the machine and it is valid whether it is a motor or a generator

Normaly, e and P_0 depend on the rotational speed ω_m. It is assumed here that theses values are constants.

The parameters identifications of the motor and generator have been performed by measuring the torque (T_m), the rotational speed (ω_m) and the electrical power (P_e) on the DC bus (before the power converter).

The identification of e and P_0 is straightforward as shown in Fig. III-C where the functions $P_m = f(P_e)$ (Fig. 8(a)) and $P_e = f(P_m)$ (Fig. 8(b)) are plotted for the motor and generator, respectively.

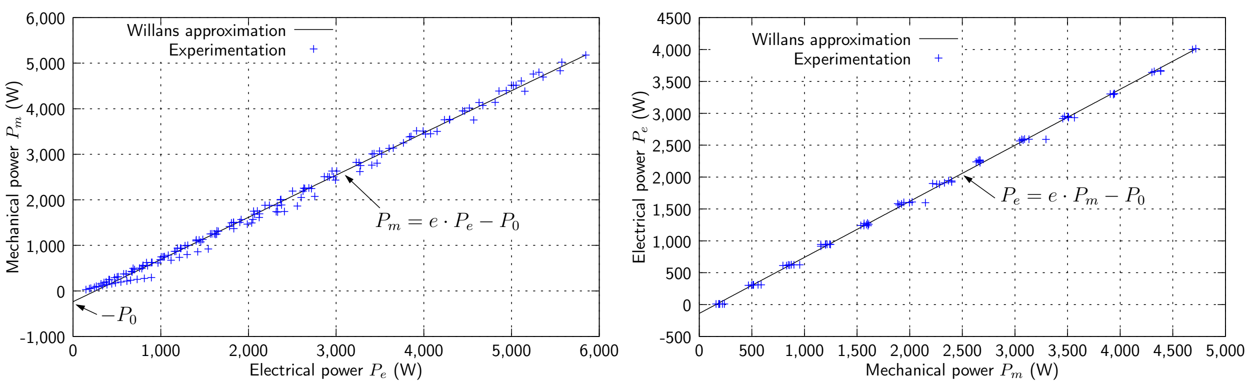

(a) Willans approximation of the motor drive

(b) Willans approximation of the generator drive

Figure 8. Approximation de Willans de la gnratrice et des convertisseurs associs

D. *Lead-acid batteries model*

The purpose of the battery simulations is to be able to predict the performance of the wheelchair, in terms of range, acceleration, speed, etc. For this system, the speed of the vehicle changes fairly slowly, and the dynamic behaviour of the battery is not significant. Therefore, in this paper, only the basic equivalent circuit of a battery (capacitance with a serie resistance) is used.

1) Open circuit voltage: The batteries used in the system are lead-acid batteries: the open circuit voltage E is approximatively proportional to the state of charge of the battery [7]. Considering the variable DoD, representing the depth of discharge equal to zero when the battery is fully charged and one when empty, then the simple formula (only valid for lead-acid batteries) for the open circuit voltage is [7]:

$$E = n\,(2.15 - DoD \cdot (2.15 - 2.00)) \tag{13}$$

where n is the number of cells in the battery.

2) Capacity: The capacity of a battery is reduced if the current is drawn more quickly: drawing 1 amperes for 10 hours does not take the same charge from a battery as running 10 amperes for 1 hour.

This phenomenon has to be taken into account for such an application to be able to predict autonomy of the wheelchair. Moreover, it is important to be able to predict the effect of current on capacity for the design process but also to measure the charge left in the battery.

For this application, the Peukert model the battery behavior is used [7]. This model is not very accurate at low currents but for high currents it models the battery behaviour well enough.

The Peukert capacity (C_p) is calculated as follows :

$$C_p = I^k\,T \tag{14}$$

where k is constant called the Peukert coefficient (arround 1.2 for lead-acid batteries). The Peukert capacity is equivalent to the normal ampere-hours capacity for a battery discharges at 1 A.

If the capacity is given, for example, for $T = 10$ hours, the Peukert capacity will be calculated as follows :

$$C_p = \underbrace{\left(\frac{C_{10}}{10}\right)}_{I}{}^{k} \cdot 10 \tag{15}$$

If a current I flows from the battery, then, from the point of view of the battery capacity, the current that appear to flow out of the battery is I^k. Therefore, the capacity which is removed from the battery is:

$$C_R\ [\mathrm{Ah}] = \int \frac{I^k}{3\,600}\,\mathrm{d}t \tag{16}$$

The initial condition of C_R have to be given for the simulation :

$$C_{R,\mathrm{init}} = C_p \cdot DoD_{\mathrm{init}} \tag{17}$$

where DoD_{init} is the initial depth of discharge.

3) Depth of Discharge: The depth of discharge of the battery is the ratio of the charge removed to the original capacity:

$$DoD = \frac{C_R}{C_p} \tag{18}$$

The calcultated value of DoD is used to compute the open circuit voltage given by (13).

E. Supercapacitors

The supercapacitors are modeled using an equivalent electrical circuits given in the figure 9.

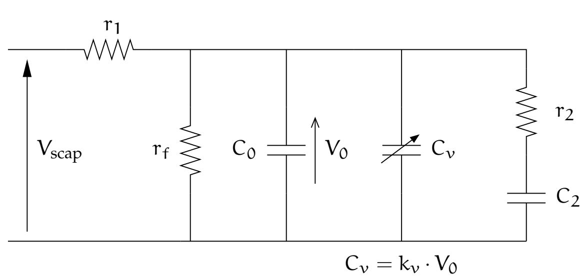

Figure 9. Equivalent models of supercapacitors

In this model, several parts can be distinguished:

- *The main branch* containing the resistance r_1 and the capacitances C_0 and C_v. This branch determines the energy evolution during charge and discharge cycles. C_v varies as a function of its voltage: $C_v = k_v \cdot V_0$;
- *The slow branch* containing the resistance r_2 and the capacitance C_2. This branch models the inernal charge redistribution at the end of the charge or discharge process;
- *The resistance* r_f which models the self discharge branch. The numerical value of r_f is in the order of some kilo-ohms.

For this application, r_f is neglected as high current dynamic is imposed to the ultracapcitors.

IV. Simulation and experimentation

A. Engine only configuration

The figure 10(a) shows the DC bus current distribution between the load, the battery and the generator coupled to the engine. The generator gives almost all the current to the load. The battery works only during small transient phases, when the generator is at his maximum power ($t = 75$ seconds) and during the braking period ($t = 135$ seconds). The fuel consumption during the tested cycle was about 88 grams.

B. Battery hybridization configuration

The tests results of the battery configuration is shown in figure 10(b). It can be seen that the DC current generator is more smoothed than in the previous case (figure 10(a)). The battery gives transient phases and recovers energy during the braking. With this control strategy, the fuel consumption is 73 grams (18 percent less).

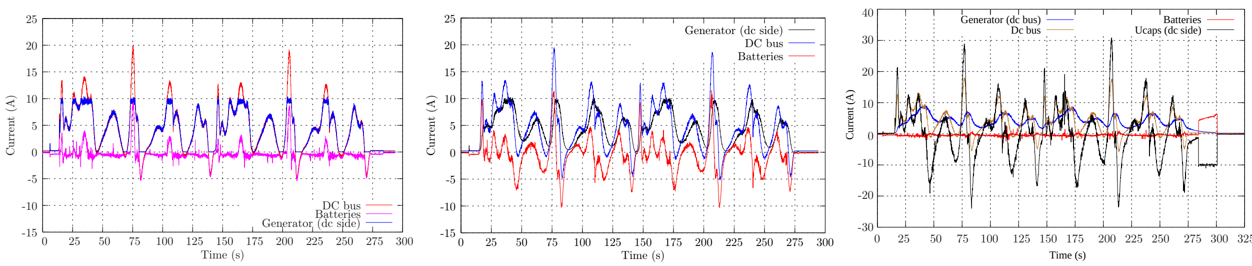

(a) Engine only configuration (b) Battery hybridization configuration (c) Battery-ultracapacitors hybridization configuration

Figure 10. Expeirimental DC bus currents

C. Ultracapacitors hybridization configuration

The results are shown on figure 10(c). The battery current is about zero during the cycle. At the end of the cycle it can be seen that the battery charges the ultracapacitors. Of course, this can be optimised in order to manage the ultracapacitors voltage during the cycle. In this configuration, the generator DC current (i.e., engine power) is very low: its maximum current is never reached.

In this case the consumption is about 72 grams (about the same consumption with the battery hybridization). Despite this configuration does not add significant fuel economy, the battery transients is limited. This configuration can help to improve the batteries lifetime because of less dynamic sollicitations (charge/discharge cycles).

The ultracapacitors voltage (figure 11), never goes under 110 volts (the maximum voltage is about 150 volts).

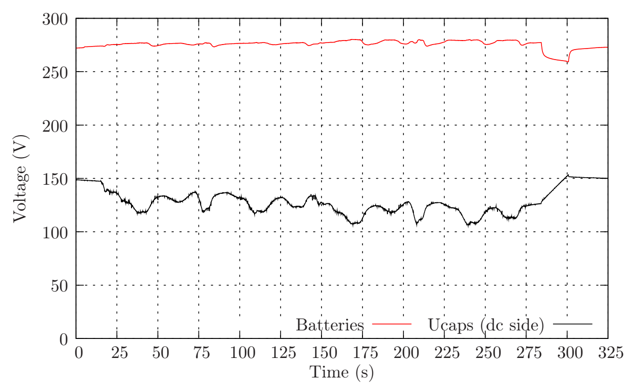

Figure 11. Battery and ultracapacitors voltages

D. Simulation and experimental comparison

The models have been validated separately and have been coupled in order to simulate several architecture with their energy management before testing them on the tests bench.

Simulations are easier and permit to save time in the development of new control strategies. The three configurations have been simulated under the same experimental driving cycle.

The simulation results show that the models are accurate and that the energy management works correctly and gives expected results.

The thermal engine associated with the generator model works well. Some differences can be seen between the simulated and experimental engine mechanical torque (figures 12(a), 12(b) and 12(c)) but the Willans approximation still gives very good results.

	Simulation	Experimentation
Engine only	74	88
Battery hybrid	68	73
Utracaps/battery hybrid	64	72

Table II
EXPERIMENTAL AND SIMULATED FUEL CONSUMPTION (IN GRAMS)

The table II shows a comparison bewtween the predicted (simulation) and actual (experimental) fuel consumption. The differences between the simulated and experimental consumption are mainly due to the engine model which only predict steady state operating points without taking into account transients where the consumption can be very different. A dynamic engine model can improve these simulation results.

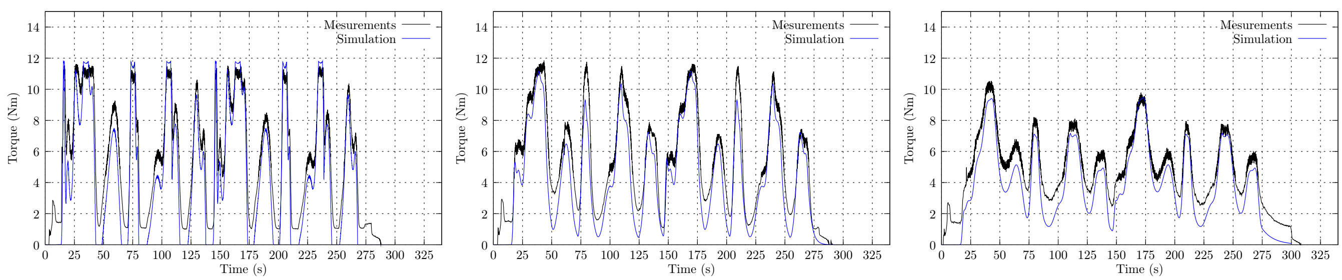

(a) Engine mechanical torque - (engine only configuration)
(b) Engine mechanical torque - (battery hybridization configuration)
(c) Engine mechanical torque - (battery-ultracapacitors hybridization configuration)

Figure 12. Simulated and experimental engine torque

The battery model does not predict perfectly the actual voltage (figure 13) because the Peukert model does not take into account the high double layer capacitance of gel lead batteries. Normally simple lead acid batteries are used instead of gel lead acid batteries: in this case the voltage prediction and battery state-of-charge is more accurate with such a model.

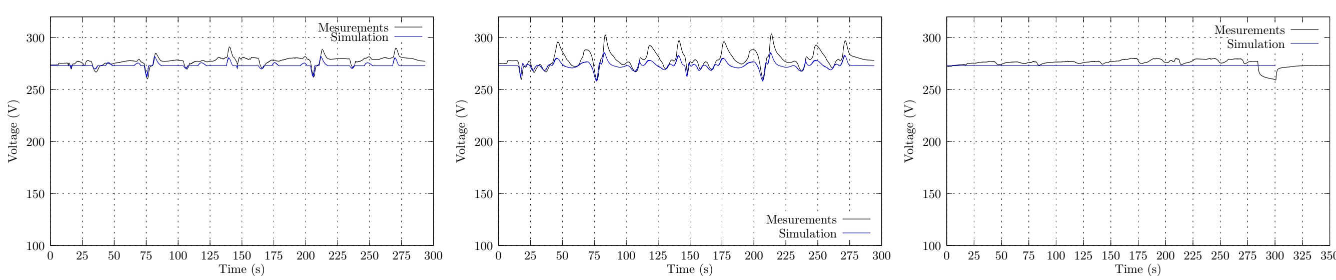

(a) Batteries volatage - (engine only)
(b) Batteries volatage - (battery hybridization)
(c) Batteries volatage - (battery-ultracapacitors hybridization)

Figure 13. Simulated and experimental batteries voltages

As shown in figure 14 The ultracapacitors voltage is very well predicted all along the driving cycle.

V. CONCLUSION

This paper present a simulation and experimental comparison study of three HEV series architectures: engine only, battery hybridization and battery-ultracapacitors configurations. The models of the components, including vehicle, batteries, ultracapacitors, motor, generator and engine have been introduced and validated separately on the tests bench.

Simulation and experimental results show that the fuel economy in the battery configuration is about 17 % compared to the engine stand-alone solution.

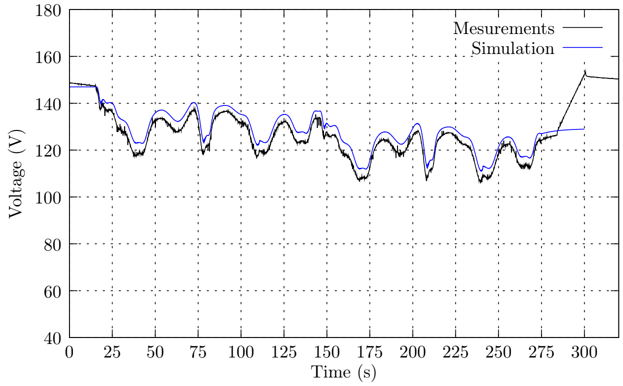

Figure 14. Simulated and experimental ultracapacitors voltages

Despite the battery-ultracapacitors configuration does not add significant fuel economy, it is shown that the battery transients can be limited to improve their lifetime. Simulation and experimental comparison show that the models permits the energy management strategies to be evaluated with a good accuracy before testing them on the real test bench.

REFERENCES

[1] B. Blunier and A. Miraoui, *Piles à combustible, Principe, modélisation et applications avec exercices et problèmes corrigés*, ser. Technosup, Ellipses, Ed., 2007, livre en français.
[2] D. Bouquain, B. Blunier, and A. Miraoui, "A hybrid fuel cell/battery wheelchair - modeling, simulation and experimentation," in *Vehicle Power and Propulsion (VPP), EEE Conference, Chine*, 2008.
[3] L. Guzzella and C. H. Onder, *Introdution to Modelin and Control of Internal Combustion Engine Systems*. Springer, 2004.
[4] L. Guzzella and A. Sciarretta, *Vehicle Propulsion Systems, Introdution to modeling and optimization*, 1st ed. Springer, 2005.
[5] M. Ehsani, Y. Gao, S. E. Gay, and A. Emadi, *Modern Electric Hybrid Electric, and Fuel Cell Vehicles, Fundamentals, Theory, and Design*. CRC Press, 2005.
[6] K. J. Patton and J. B. Nitschke, R. G.and Heywood, "Development and evaluation of a friction model for spark ignition engine," in *Society of Automotive Engineers international congress and exposition*, no. 890836. Detroit, MI (USA): Society of Automotive Engineers, 27 Feb – 3 Mar 1989, p. 21 p.
[7] J. Larminie and J. Lowry, *Electric Vehicle Technology Explained*. John Wiley and Sons, Ltd, 2003.